

# Analysis of Prompt Excursions in Simple Systems and Idealized Fast Reactors

By W. R. Stratton, T. H. Colvin and R. B. Lazarus\*

Fast reactor accidents which are severe enough to result in a prompt neutron excursion may be divided, conveniently, into two broad classes. These are: (1) the case where the core structure is intact at the inception of the burst; and (2) the case where the core structure has lost its rigidity and is collapsing because of high temperatures and/or external forces. This paper presents a parametric study of prompt neutron bursts in solid metal assemblies and the beginning of such a study in rather idealized fast reactors. An attempt is made to present a unified picture, connecting known experiments in simple systems with large fast reactors in which experimental information is nearly nonexistent. Two methods are used to estimate the fission yields of the various prompt excursions. The first of these is coded for a fast digital computer. The generation of fission energy, the equations of motion, etc., are integrated stepwise in space and in time during the history of the burst or accident. The second is a modified Bethe-Tait<sup>1</sup> method and is suitable for estimating the "maximum credible" accidents covered under case (2) above. Comparison is made between the two methods for appropriate cases.

The paper is divided into two major sections. The first portion contains a brief description of the code, the calculation of Godiva<sup>2</sup> and similar solid metal assemblies, and the calculation of prompt bursts in idealized fast reactors, making use of two basically different assumptions. The second section contains an analysis of bursts in fast reactors making use of a modified Bethe-Tait theory. Comparison between the two methods is made where applicable.

The calculation (first method above), as coded for a fast digital computer, can be thought of as two very nearly independent parts. The first concerns the calculation of a prompt neutron  $\alpha$  and a neutron flux distribution. This has been done by either the Serber-Wilson<sup>3</sup> or the Carlson<sup>4</sup>  $S_n$  method. Of the two formulations of the problem, the Serber-Wilson scheme has been used for the entire parametric study. The  $S_n$  formulation has been used at judicious check points for comparison purposes. The two schemes usually agree, but for certain special cases the results are

divergent. Differences will be noted and discussed at the appropriate point below. These formulations of the fast neutron diffusion problem have been described elsewhere and will not be discussed further in this paper.

The second portion of the code is concerned with the generation of fission energy and the description of the dynamics of the problem in space and time. The code applies only to spherical geometry. If a problem is encountered that has been performed in, for example, cylindrical geometry, a suitable spherical analogue must be found. Some justification for this procedure can be found in "shape factor" experiments described by H. C. Paxton<sup>5</sup> where the critical volumes of cylinders are compared to those of spheres.

For calculational purposes the spherical assembly is divided into a number of hypothetical spherical shells or mass points. Each mass point may be characterized by various constants, nuclear and otherwise, such as transport and fission cross sections, neutrons per fission, mass, volume, etc. The neutron flux is then a step function in radius, since the various quantities characterizing a mass point are considered constant throughout the region represented by the mass point. The number of mass points used in a problem is usually between ten and twenty and is a function of the complexity of the problem.

The bookkeeping system used to identify variables in space and in time is most easily explained by the following examples:  $R_i(t)$  refers to the radius  $i$  ( $i = 1, 2, \dots, I$ ) at the time  $t$  ( $\mu\text{sec}$ ) in the problem.  $R_I$  (cm) is the outer boundary of the assembly and  $R_1$  is the interface bounding the innermost mass point.  $\theta_{i-1/2}(t + \Delta t)$  is the temperature (volts) of the mass  $M_{i-1/2}$  (grams) located between radii  $R_{i-1}$  and  $R_i$  at the problem time  $t + \Delta t$ .  $\Delta t$  is the time interval used in the stepwise time integrations.

The calculation is necessarily performed on a cyclical basis. To describe the equations used, and the method of advancing the problem cyclically, assume that the following variables are known: interface radii,  $R_i(t)$ ; velocities,  $\dot{R}_i(t - \Delta t/2)$ ; accelerations,  $\ddot{R}_i(t)$ ; neutron flux,  $\phi_{i-1/2}(t - \Delta t/2)$ ; and material temperatures,  $\theta_{i-1/2}(t)$ . The dot notation ( $\dot{R}$ ,  $\ddot{R}$ , etc.) implies the time derivatives of the variable. The problem is advanced one cycle in time in the following manner,

Contributors: E. W. Salmi and R. Canada.\*

\* University of California, Los Alamos Scientific Laboratory, New Mexico.

fundamentally quite simple. The interface velocities are advanced first:

$$\dot{R}_i(t + \Delta t/2) = \dot{R}_i(t - \Delta t/2) + \ddot{R}_i(t)\Delta t. \quad (1)$$

These velocities are used to advance the radii:

$$R_i(t + \Delta t) = R_i(t) + \dot{R}_i(t + \Delta t/2)\Delta t. \quad (2)$$

The total neutron flux can be advanced in time by

$$\phi_{i-\frac{1}{2}}(t + \Delta t/2) = \phi_{i-\frac{1}{2}}(t - \Delta t/2)e^{\alpha(t)\Delta t} \quad (3)$$

since  $\alpha$  at the cycle  $t$  is a function only of the geometry and material. It is obtained from the  $S_n$  or Serber-Wilson calculation, along with a new spatial distribution. Given a new flux density (and distribution), the fission energy rate (per gram) is obtained easily:

$$\begin{aligned} \dot{E}_{i-\frac{1}{2}}(t + \Delta t/2) \\ = \epsilon \Sigma_f \phi_{i-\frac{1}{2}}(t + \Delta t/2) \\ \times V_{i-\frac{1}{2}}(t + \Delta t/2) \end{aligned} \quad (4)$$

where  $\epsilon$  is the energy release per fission ( $= 178$  Mev),  $\Sigma_f$  ( $\text{cm}^{-1}$ ) is the material macroscopic fission cross section, and  $V$  is the specific volume ( $\text{cm}^3/\text{gm}$ ). Given the fission energy rate, one may simply sum in space and time to obtain the total energy release.

It has been found useful (although not necessary) to make use of a temperature dependent equation of state. If we assume that the fission energy generated in mass point  $i - \frac{1}{2}$  in the cycle interval  $\Delta t$  is deposited as internal energy, except for the thermodynamic work this mass point performs on its neighbors, we advance the temperatures (energy units) by

$$\theta_{i-\frac{1}{2}}(t + \Delta t) = \theta_{i-\frac{1}{2}}(t) + \dot{\theta}_{i-\frac{1}{2}}(t + \Delta t/2)\Delta t \quad (5)$$

where

$$\begin{aligned} \dot{\theta}_{i-\frac{1}{2}}(t + \Delta t/2) = \frac{1}{C_{i-\frac{1}{2}}(t + \Delta t/2)} \left[ \dot{E}_{i-\frac{1}{2}}(t + \Delta t/2) \right. \\ \left. + \theta_{i-\frac{1}{2}}(t) \left( \frac{\partial P}{\partial \theta} \right)_{i-\frac{1}{2}}(t) V_{i-\frac{1}{2}}(t + \Delta t/2) \right]. \end{aligned} \quad (6)$$

In Eq. (6), an error has appeared in that  $C$  (heat capacity),  $\theta$  (temperature), and  $\partial P/\partial \theta$  ( $P =$  pressure) should be at the time  $t + \Delta t/2$  rather than at time  $t$ . The error is small and may be remedied if so desired. Given new temperatures, the pressures are given by some suitably defined equation of state:

$$P_{i-\frac{1}{2}}(t + \Delta t) = P_{i-\frac{1}{2}}(\theta_{i-\frac{1}{2}}(t + \Delta t), V_{i-\frac{1}{2}}(t + \Delta t)), \quad (7)$$

and new accelerations are simply obtained:

$$\begin{aligned} \ddot{R}_i(t + \Delta t) = \frac{4\pi R_i^2(t + \Delta t)}{M_i} \\ \times [P_{i-\frac{1}{2}}(t + \Delta t) - P_{i+\frac{1}{2}}(t + \Delta t)]. \end{aligned} \quad (8)$$

In Eq. (8),  $M_i$  is a suitably defined mass associated with the radius  $R_i$ . The problem has been advanced one cycle and the calculation is returned to Eq. (1) to start a new cycle.

Typical problems may have between 500 and 1500 such cycles. The number of cycles depends in part upon the complexity of the problem. Generally, the neutron calculation is performed only one cycle in five. Prompt alphas and flux distributions are extrapolated by means of a quadratic function on cycle number  $t$ . In general, one can watch the rise and fall

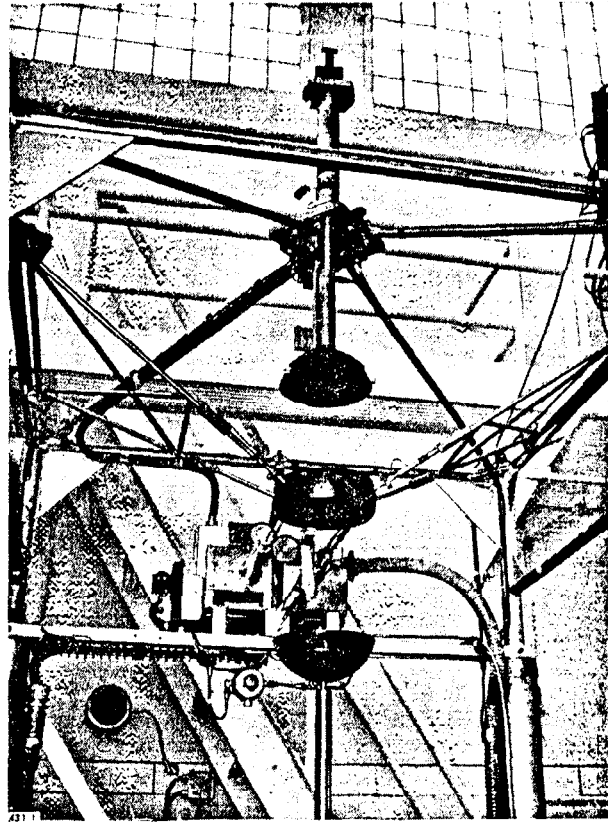


Figure 1. Godiva in the disassembled state. The central section is fixed in position by small steel supports while the upper and lower sections are retractable by means of pneumatic cylinders.

of variables such as fission rate, temperatures, pressures, velocities, densities, etc., in space and in time.

The first problem to which this code was directed was the series of controlled and instrumented prompt bursts in the Godiva assembly.<sup>2, 6</sup> Godiva consisted of three pieces of enriched (93.7%  $\text{U}^{235}$ ) uranium which were assembled by remote control in the form of a sphere whose total mass was about 55 kg. There was no reflector. Prompt neutron bursts were initiated experimentally by rapid insertion ( $5 \times 10^{-3}$  to  $30 \times 10^{-3}$  seconds) of an enriched uranium rod into the center of Godiva. Godiva, in an unassembled state, is illustrated in Fig. 1.

The measurements associated with the various bursts were total fissions occurring in the "spike" or prompt excursion, the maximum fission rate, the width of the spike, in time, at one-half the maximum value, and the period ( $= 1/\alpha$ ) or  $e$ -folding time of the neutrons in the assembly. The first three of these quantities are illustrated in Figs. 2, 3, and 4, respectively. The energy release in the most supercritical burst (about 8.5 cents over prompt critical) was 0.18 lb high explosive equivalent ( $1 \text{ lb} = 7.4 \times 10^{16}$  fissions). Two accidental bursts have occurred of yield magnitude  $6 \times 10^{16}$  fissions and  $1.2 \times 10^{17}$  fissions.

The calculation was normalized to the Godiva assembly by adjusting the nuclear constants until a prompt alpha of zero was calculated for the prompt

critical mass, and a prompt alpha of  $-1.03 \times 10^6$ /sec was calculated for the delayed critical mass.<sup>7</sup> Given such a normalization, there remained only determination of an equation of state. The function which enabled us to calculate the Godiva results is:

$$P = a + b\theta + c\rho, \quad (9)$$

where  $P$  is in megabars,  $\theta$  in volts, and  $\rho$  in grams/cm<sup>3</sup>.  $a$ ,  $b$ , and  $c$  are given by  $-0.545649$ ,  $0.27846$ , and  $0.02873$ , respectively. This function is undoubtedly not unique, but to date we have found no satisfactory substitute. The uranium heat capacity (used in Eq. (6)) is well known.<sup>8</sup>

Given the above conditions, a number of problems were run representing bursts of various reactivities in Godiva. The starting reactivity was varied by adjusting the mass of the outermost mass point. The results in terms of total fissions, maximum fission rate and pulse width are illustrated in Figs. 2, 3, and 4, respectively, superimposed on the experimental results.

It can be seen (Fig. 2) that the experimental burst yields for various excess reactivities are matched satisfactorily except for the lowest reactivities where the calculated results are low by a small amount. The significant point to note is that the yield is linear with excess reactivity for low reactivities, but that at about four cents over prompt critical, a "break" occurs and the fission yield commences to rise much faster. The calculated results match this "break" quite accurately. The "break" occurs at that excess reactivity where the system is no longer in mechanical equilibrium. That is, for high reactivities, energy is being generated faster than the system can expand to return to equilibrium.

The calculated maximum fission rates miss the experimental values (Fig. 3) by small amounts at both extremes of reactivity; and the burst widths (Fig. 4) are low by about 15% at the higher reactivities. None of these small differences is considered significant. Figure 5 shows the individual bursts.

Given the satisfactory agreement with the Godiva experiments, a series of calculations was made on other Los Alamos Scientific Laboratory critical assemblies. In particular, Rossi alpha measurements<sup>7</sup> exist for bare uranium assemblies of 29% and 54% enrichment and for Topsy, a reflected uranium assembly whose core was enriched to 93.7% U<sup>235</sup>. Burst calculations were made for these assemblies in the same manner as was done for Godiva. The same equation of state was used, but different nuclear constants were, of course, required to force agreement with critical masses and Rossi alphas. Some of the results of these calculations are illustrated in Fig. 6. In this figure, we have plotted total fissions divided by core mass as a function of the initial reactivity above prompt critical. The unreflected assemblies reduce to a common linear relationship below about four cents excess reactivity; the "break" from a linear relationship with excess reactivity occurs at

very slightly higher reactivities for the assemblies of lower U<sup>235</sup> content. The fission density is higher in Topsy at low reactivities.

A number of calculations have been made for hypothetical reflected assemblies of varying core U<sup>235</sup> enrichment and reflector thickness. In general, for fixed excess reactivity and a core of 94% U<sup>235</sup>, one can construct a smooth sequence of fission densities varying somewhat less rapidly than the first power of the reflector thickness between the limits defined by Godiva and Topsy. Bursts calculated for reflected assemblies whose cores have lower U<sup>235</sup> enrichment follow this same general pattern. These data and the data on Fig. 6 may be thought of as representing a scaling law connecting prompt burst energies of various spherical "solid" assemblies whose construction is similar to that of Godiva.

An additional result that can be obtained from these calculations is the kinetic energy contained in the moving metal as the assembly expands to relieve internal pressures. Clearly this quantity is zero after a controlled excursion. However, if the metal should rupture or if parting planes exist, the energy converted to this form should be readily recognized. It is, in fact, the energy available to do damage in an accident. In general, the calculation shows this quantity rising to a maximum, and (usually) dropping after the fission rate goes to a low value. For illustrative purposes we have chosen the maximum kinetic energy generated as a number with which to work. In terms of accidents, this is obviously the most pessimistic case. The ratio of this energy to the total energy release is illustrated in Fig. 7 for Godiva and for the bare assembly of 29% U<sup>235</sup>. Two other assemblies are illustrated which

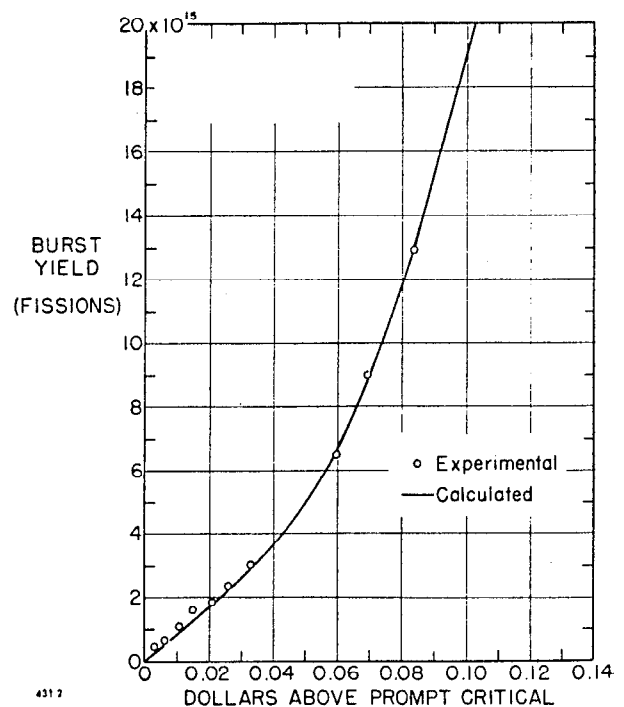


Figure 2. Godiva burst yield versus initial excess reactivity

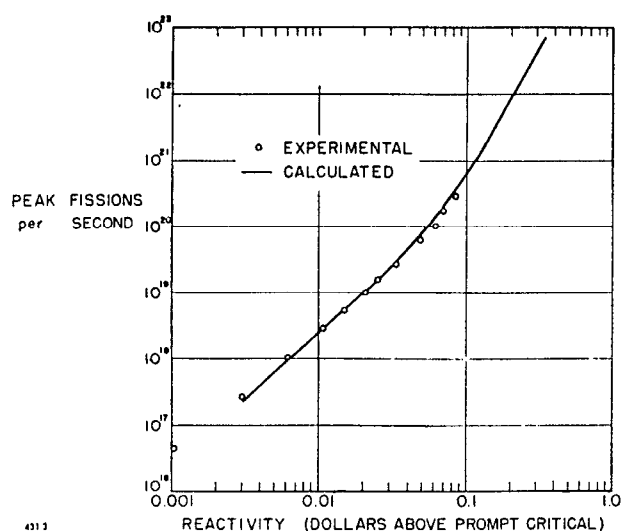


Figure 3. Peak fission rates during Godiva prompt bursts for various initial excess reactivities

are discussed below. The fraction of the fission energy that is converted to kinetic energy in the solid metal assemblies is evidently quite small for bursts of less than about 20 cents. The absolute values of these ratios are not as accurate as the data presented in Figs. 2, 3, 4, 5, and 6. The ratios may be low by a factor somewhat less than two.

The only experimental check one has on this quantity for fast neutron systems† is the Godiva accidental prompt burst of February 12, 1957. This burst of  $1.2 \times 10^{17}$  fissions was equivalent to about 1.7 lb H.E. However, as illustrated in Fig. 8, the damage done to Godiva was very slight, not at all equivalent to that which would have been caused by 1.7 lb H.E. Some warping of the pieces occurred, the central rod was stretched and finally ruptured, and considerable oxidation is evident. From these photographs it is apparent that the central temperatures were very close to the melting temperature. To calculate a burst which agrees with the measured yield of  $1.2 \times 10^{17}$  fissions, an excess reactivity of about 20 cents or a period of  $5 \mu\text{sec}$  must be assumed. From Fig. 7, it is seen that at its maximum, the kinetic energy was only about 1.4% of the total energy release. This relatively small amount (0.024 lb H.E.) of damage energy is much more consistent with the observed damage than is 1.7 lb H.E. The calculated central temperatures are about  $50^\circ\text{C}$  short of the uranium melting point. Most of the fission energy was deposited as heat content.

The assemblies discussed above have been relatively simple. The calculated results are thought to be accurate and are simple to interpret. The question exists as to how accurately such a calculation can be made to represent a prompt excursion in a complicated

† The final excursion of the Borax I water moderated reactor<sup>9</sup> gives some information on this question. The total fission energy created during this excursion was about 65 lb H.E. equivalent. It has been estimated that between 6 and 17 lb of TNT would have produced comparable damage.

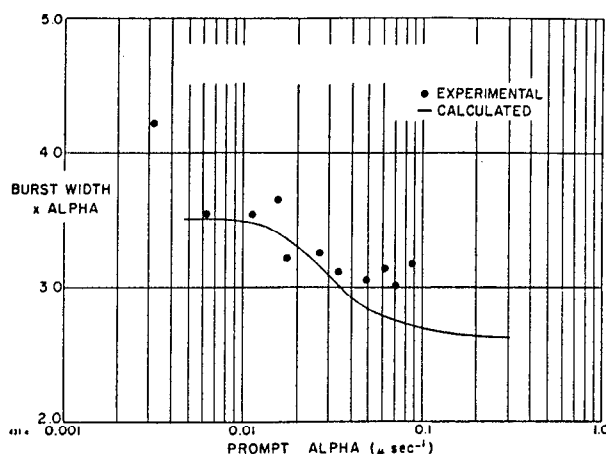


Figure 4. Width of the prompt burst in time at one-half maximum times the prompt alpha versus the initial prompt alpha

The high experimental point at  $\alpha = 0.0031 \mu\text{sec}^{-1}$  may have been caused by neutrons reflected from the ground and supporting structure

assembly such as a fast reactor. We wish to calculate, for example, a system consisting of pins of enriched uranium, perhaps canned with a nonfissile substance. This critical system of pins may or may not be immersed in a cooling fluid such as sodium or NaK. A reflector of some similar design will also exist. We wish to calculate the fission energy released when this assembly, for some reason, goes above prompt critical.

To attempt to calculate the dynamics of such a system, we must first construct a spherical analogue of a reactor, as our computational scheme is set for this geometry. There are two ways we can do this, neither one of which is entirely satisfactory.

We can (1) distribute the mass uniformly at an average low density and assign the material a non-linear equation of state which simulates heterogeneity, or (2) imagine the mass to be distributed in a series of spherical shells of normal density and normal equation of state. These normal density shells are to be separated by spherical shells that are essentially voids, or filled with very low density material.

The first case is similar to the model considered by Bethe and Tait.<sup>1</sup> According to this model, an accident or prompt burst has the characteristic that is generally referred to as threshold. One essentially assumes that the core structure is destroyed and that the change of reactivity with temperature ( $\Delta k/^\circ\text{C}$ ) is zero until temperatures are high enough to create positive pressures and initiate disassembly.

The second case is somewhat more realistic in that the active material is initially at normal density. In this case there is no threshold; a quenching mechanism is initiated as soon as temperatures begin to rise appreciably. The temperature coefficient of reactivity is defined by the equation of state and by the neutron calculation used. Inertial effects may be important early in the problem.

The creation of this model was prompted by the existence and flexibility of the code, of course, but also by noting how little Godiva actually expanded

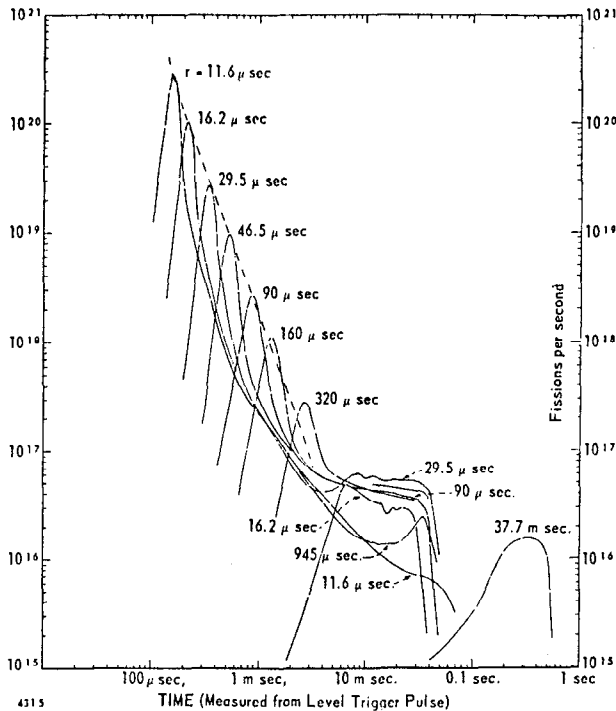


Figure 5. Godiva measured fission rate for several controlled, prompt excursions

The period ( $\tau$ -folding time) is shown for each excursion

during the quenching of a prompt burst. For a sufficiently large number of mass points, it is expected that the two models should predict yields of about the same magnitude since it is known from perturbation theory that the reactivity difference between a homogeneous and a granulated core tends toward zero as the grain size is diminished. Some computations related to this assertion are in progress, but have not been completed. For a manageable number of regions (10-20) the two models give divergent results, as will be seen below.

The problems described below are based on the calculation of the Godiva prompt bursts and the several critical experiments that have been done at the Los Alamos Scientific Laboratory. The calculational scheme has not been changed except for an extension of the equation of state. Provision has been made for densities greater than normal, the metal to liquid phase change, and finally a phase at low densities by use of a Van der Waals' function. Following Brout,<sup>10</sup> we assume a critical temperature of 14,000°K, and a critical volume of 40 cm<sup>3</sup>/mole. We accept a critical pressure of  $1.0899 \times 10^{10}$  dynes/cm<sup>2</sup>.

The first model to be set up for calculation was a bare assembly of about 66 kg of highly enriched (94% U<sup>235</sup>) uranium. This particular case was chosen to study an assembly only moderately different from Godiva in mass, with no reflector, but with a radically different geometry. The desire, of course, was to see what fission yields would result from calculated bursts making use of the two models (layered and threshold). The threshold case was set up by assuming the entire core to be at a uniform density of 0.9 that of normal

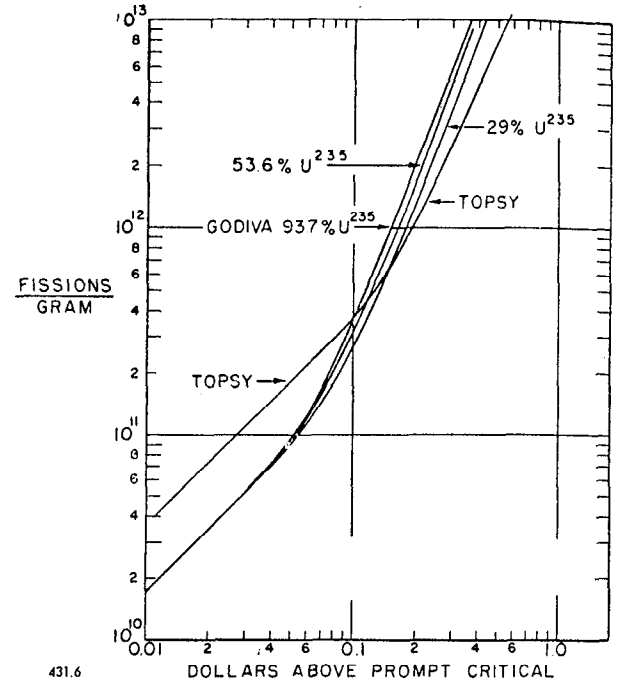


Figure 6. Calculated fission densities versus initial excess reactivity for several solid metal assemblies

Topsy was a reflected uranium assembly whose core was enriched to 93.7% U<sup>235</sup>. The other three assemblies were bare

uranium. Various excess reactivities were obtained by small changes in the mass. Bursts were then calculated as for Godiva. The burst behavior, however, was different in that a temperature rise of 1100°C was necessary before internal core pressures became greater than zero. The calculated yields were considerably greater than those calculated for Godiva. The layered case was set up by imagining the 66 kg to be in a series of mass points (spherical shells) at normal density and equal thickness. These mass points were separated by regions of low density material (normal uranium at a density of 2 grams/cm<sup>3</sup>). Dynamically, the dense regions were separated by voids. Prompt bursts were effected by adjustments in the mass of the outer shell.

The prompt bursts for this core, as calculated by use of the threshold and layered assumptions, are displayed in Fig. 9 along with those of Godiva for comparison. The data are presented in terms of fission energy density versus initial reactivity above prompt critical.

The third assembly in this figure is discussed below. It can be seen that the fission energy density for the layered case is about three times that of Godiva for low excess reactivities (linear region). However, the threshold case is higher by a factor of at least 50 and as much as 400, depending on the reactivity. For very high reactivities ( $\sim \$1$ ) the difference is more like a factor of 10, and in a limit of very high reactivities, the two models probably agree.

Additional layered cores have been set up of 95 kg and 210 kg of 94% U<sup>235</sup> and 246 kg and 540 kg of 54% U<sup>235</sup>. The average densities of these cores were

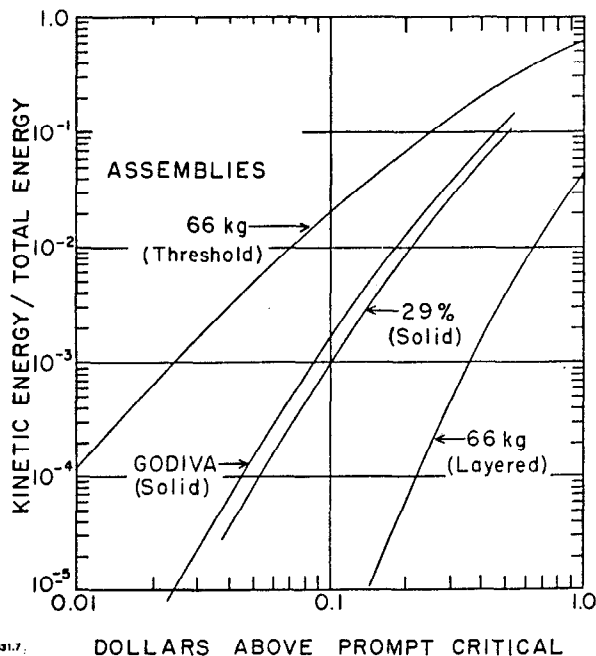


Figure 7. Calculated kinetic energies divided by total energy release versus initial excess reactivity for three assemblies. Godiva and the 29% assembly are assumed to be solid spheres. Bursts have been calculated for the 66 kg (94%  $U^{235}$ ) bare assembly by making the threshold assumption (upper curve) and the layered assumption (lower curve).

nominally 75% and 50% of normal density for the smaller and larger masses, respectively. Bursts were calculated for these assemblies in an entirely analogous manner. The fission energy densities of these bursts, as a function of reactivity, fall fairly close to, but slightly higher than, the 66 kg case described above. The most extreme case, that of 540 kg of 54%  $U^{235}$ , was greater than the 66 kg case (above) by a factor of two. Apparently the scaling laws illustrated in Fig. 6 hold, at least within the accuracy of the calculation.

The third assembly illustrated in Fig. 9 has a core of 147 kg of highly enriched (94%  $U^{235}$ ) uranium and a reflector of normal uranium. The core was  $\frac{1}{2}$  normal density for the threshold case and slightly less than  $\frac{1}{2}$  on the average for the layered case. The reflector was layered for both cases. Prompt bursts were effected by small adjustments in the mass of the outermost core mass point. The temperature rise for positive pressures to become significant in the threshold case was about 4000°C. Again the two assumptions give divergent results at low reactivities.

Further information of interest can be gleaned from the calculational results representing these bursts. The fraction of the total fission energy that is converted to energy of motion is illustrated in Fig. 7 for the bare 66 kg assembly discussed above along with Godiva results for comparison. The layered case is lower because of the lower yields, but also because internal pressures are invariably lower for the same energy density. Evidently, each individual shell can expand and consequently relieve its internal pressures much more easily than can a solid assembly acting

more as a unit. This point is further illustrated by reference to Fig. 9. It can be seen that the linear region of yield (for the layered cases), as a function of reactivity, extends to much higher reactivities than does the curve representing Godiva. The layered assemblies are able to maintain mechanical equilibrium for more violent bursts than can Godiva. As was mentioned previously, the calculated kinetic energies are thought to be low by as much as a factor of two. However, relative values should be good.

A significant difference between the Serber-Wilson and  $S_n$  methods first appears in the above discussed layered problems. The  $S_n$  and Serber-Wilson methods predict very closely the same variation in  $\alpha$  during a burst calculation of a solid assembly, but the  $S_n$  predicts a significantly smaller  $\Delta z$  during the burst calculation of a layered problem than does the Serber-Wilson method. Selected check points suggest that the change in  $\alpha$  for a given change in configuration is smaller in the  $S_n$  calculation by a factor of between 2 and 4, depending on the problem. This interesting result can be interpreted as saying that the two methods give different temperature coefficients of reactivity for layered models, but the same coefficient for homogeneous models. Since the calculated yield is inversely proportional to this coefficient, it is expected that the yields of the layered problems in Fig. 9 would be raised by factors of between 2 and 4, if the  $S_n$  code were incorporated in our calculation. Although this indicates the importance of the neutron calculations for quantitative yield predictions of a given reactor model, the qualitative difference in yields between the homogeneous and layered models remains unaffected.

A second perturbation in the results can be created by examination of the equation of state (Eq. (9)). This equation of state predicts a compressibility of uranium, for example, that is lower than published values by a factor of about two. This inconsistency can be removed by raising the coefficient of  $\rho$  (with a corresponding change in the constant term so as to

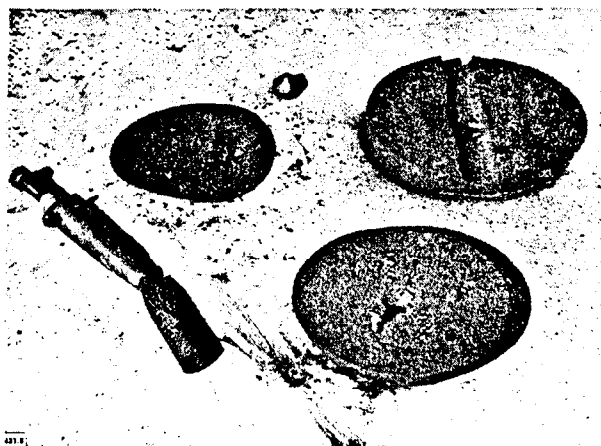


Figure 8. View of several pieces of the Godiva assembly after the accidental burst of February 12, 1957. The energy release during this excursion was equal to 1.7 lb H.E. equivalent.

retain zero pressure for room temperatures and normal density). The net result is that, approximately, the calculated yields are raised by the same factor we used to raise the coefficient of  $\rho$ . We have now abandoned the normalization to Godiva, of course. If we should now raise the coefficient of  $\theta$  by about the same factor (so as to preserve, for example, the coefficient of volume expansion), the yields are returned, again approximately, to their original values. However, the Godiva results are not restored with the accuracy indicated in Figs. 2, 3 and 4, by this second change, and apparently cannot be with any such simple change in the equation of state.

One can go a step further and construct an equation of state, which, with a given neutron code, directly reflects the temperature coefficient of reactivity of the reactor of interest. Here one must consider only those core materials of direct interest. For example, the time scale of a prompt burst in a fast system is generally so short that very little heat would flow from uranium rods to a coolant. The most pertinent coefficient in, for example, the EBR-II<sup>11</sup> may be the linear coefficient of expansion of the core pins. The value for this part of the core is about 1/3 that calculated for the layered, reflected core of 147 kg discussed above. If we should take an equation of state to reflect this coefficient, the calculated yields would again be about three times those illustrated in Fig. 9. This last step has about the same effect as changing to the  $S_n$  method. Both changes could not be applied at the same time.

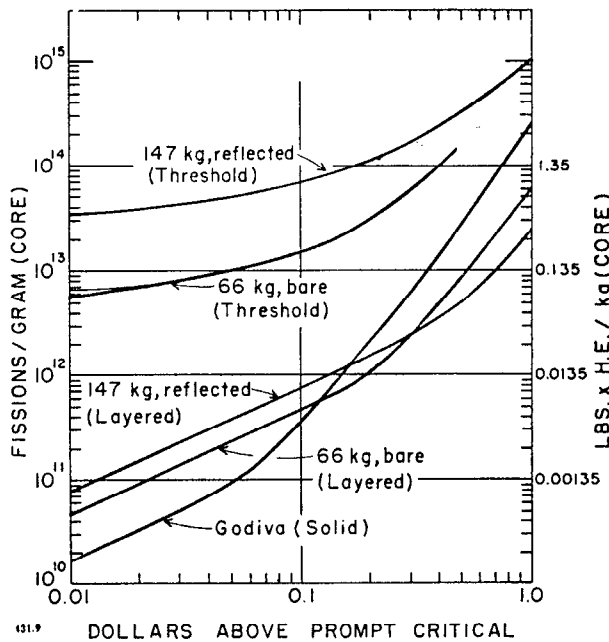


Figure 9. Fission energy densities versus initial excess reactivity for a 66 kg bare core, a 147 kg reflected core, and Godiva (for comparison)

The 66 kg and the 147 kg cores are assumed to be made of uranium enriched to 94%  $U^{235}$ . The upper two curves represent bursts obtained by assuming a threshold model, while the lower two represent bursts obtained by assuming a layered model

The uncertainties discussed above may be summarized by stating that we can find reasons for suspecting that our burst calculations for the layered cases may be low by a factor probably no greater than three or four. In all cases, however, the qualitative difference between the layered and threshold models remains.

The addition of reactivity to an assembly can be effectively instantaneous only in very special cases. A more likely possibility is the situation where reactivity is being added at a given rate and the neutron flux is multiplying as determined by the prompt alpha. The insertion rate is continued until an energy density is achieved which initiates some quenching mechanism. The burst then proceeds from the point of maximum reactivity in a manner analogous to those assemblies which suffered a step-function increase in reactivity. The procedure used to insert reactivity in this study is to give all radii negative velocities at the problem start time. The initial prompt alpha is zero, and the power level is set at some arbitrary level, usually about one megawatt. The rate of change of reactivity caused by the material collapsing inward is determined by the initial velocities.

The same threshold and layered cases studied above were examined. Bursts were initiated by collapsing the core at various initial velocities. Typical initial velocities were 0.32, 3.2, 10 and 32 ft/sec. The resulting burst yields are displayed in Fig. 10 as a function of the initial reactivity insertion rate. The same pattern is evident in this figure as was seen in Fig. 9. In fact, if the results of these calculations are plotted in Fig. 9 against the maximum reactivity attained during the problem, the points are nearly identical to those obtained from a step-function increase of reactivity. To our knowledge this fact was first discovered by Nyer *et al.*,<sup>12</sup> during analysis of the 1956 SPERT experiments.

An additional calculation has been made on the

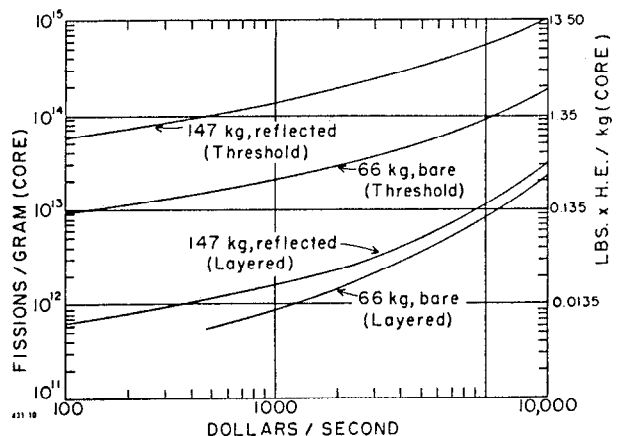


Figure 10. Fission energy densities versus initial reactivity insertion rate for a 66 kg bare core and a 147 kg reflected core

The upper two curves represent bursts obtained by assuming a threshold model, while the lower two represent bursts obtained by assuming a layered model. The initial prompt alpha was zero and the initial power level was about one megawatt

66 kg assembly. The insertion rate was identical to a previous problem, but the initial power level was lowered by a factor of  $10^6$ . This variation essentially allowed the core to collapse further and to a higher  $\alpha$  before disassembling pressures were developed. The yield was increased by a factor of 2.7. Evidently, the calculated yield is relatively insensitive to the initial power level. This point has been noted previously.<sup>1,13,14</sup>

A special problem was set up to examine, if possible, the case of a core meltdown within the limitations of the calculational method as described above. The situation imagined is that described by L. J. Koch *et al.* in their excellent description of the EBR-II.<sup>11</sup> Their statements describing the situation are repeated verbatim.

1. The sodium has boiled away from the center of the reactor.
2. The uranium from the middle part of the core has trickled down into the lower part of the core and is retained there, producing an abnormal concentration of enriched uranium at the core bottom, with a large gap at the core center.
3. At the worst possible moment, the upper portion of the core falls as a single unit, producing a prompt critical configuration at the highest possible insertion rate.

In their discussion of this situation, a reactivity insertion rate of 600 \$/sec is deduced from statement 3. Their assumption that the threshold model is applicable leads to a burst yield of 825 lb H.E. equivalent, of which 80%, or 660 lb, is expected to be available as explosive energy. (This result is stated as a "maximum credible accident." Koch *et al.* did not necessarily give credence to such an accident.)

There is some reason to suspect that the situation described above has a distinctly nonthreshold character. That is, it can be assumed that the region in the lower part of the core is a homogeneous mass, in which all empty space between pins is filled with uranium or a mixture of cladding metal and uranium. The burst behavior of this portion of the core could be much like that of Godiva. We have attempted to match the situation described above with the following set of assumptions, leading to a calculated yield.

1. We assume a core of 198 kg of uranium enriched to about 60%  $U^{235}$ .
2. 122 kg of the core material have condensed into a sphere at a density of 18.02 gm/cm<sup>3</sup>.
3. The remaining 76 kg are placed in two spherical shells about 3.5 cm and 5 cm, respectively, from the central mass of 122 kg.
4. The radii bounding these shells are initially set into motion inward at a velocity of 10 ft/sec. All other radii are initially at zero velocity. The insertion rate is 630 \$/sec.
5. These outer two shells are separated from each other, from the central sphere and from the reflector by material most like normal uranium at a density of 2 grams/cm<sup>3</sup>.

6. The initial power level was about one megawatt, and the initial prompt alpha was zero.
7. Equation (8) was modified by the addition of a constant term which was set equal to the acceleration of gravity, directed inward.

The calculated burst yield was 9.8 lb H.E. equivalent. The maximum reactivity attained during the collapse was 24.6 cents over prompt critical. This energy release is an amount expected of Godiva and in fact the fission energy density is exactly that expected of a Godiva burst 25 cents over prompt critical. It appears that the quenching was governed in large part by expansion of the central sphere. The generation of fission energy was completed in about 450  $\mu$ sec from problem start time. At this time the mass points in the central sphere were moving outward with a velocity of about 80 ft/sec. If gravity alone were operating (which is not the case) a second burst could develop in about five seconds. The calculation was not followed this far, however. To compare this result with those described above for the EBR-II, a factor of 3/2 is needed to adjust for the core mass. (The EBR-II core will have about 300 kg enriched uranium.) An additional factor of, say, 2.7 might be obtained if it is assumed that the initial power level were 1 watt rather than  $10^6$  watts. The yield could now be 40 lb, a factor of about 20 below that resulting from the threshold assumption.

The only fast reactor core meltdown on which we have information is that of the EBR-I accident of November 29, 1955.<sup>15, 16</sup> The EBR-I core consisted of

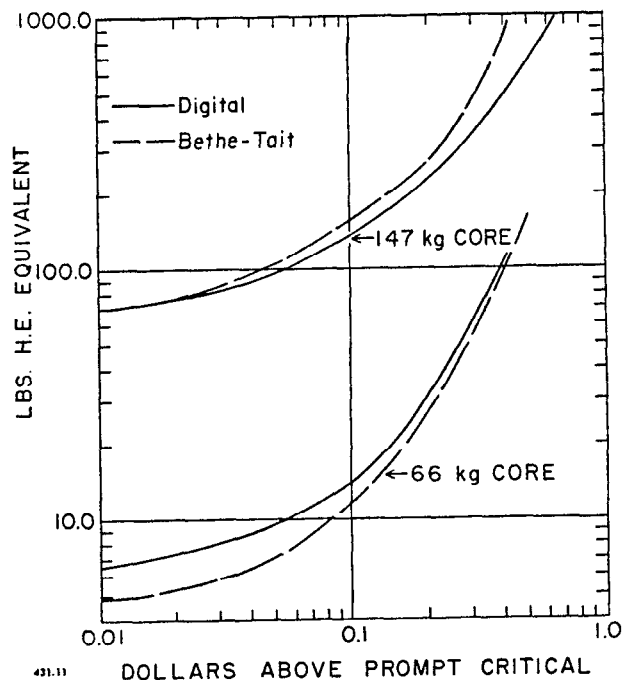


Figure 11. Fission energy release versus initial excess reactivity for two cores as obtained by two methods of estimating burst energies

The solid line represents results obtained from the calculation coded for a digital computer while the dashed line represents results obtained from a Bethe-Tait model. The threshold assumption is made in both cases

about 50 kg of uranium enriched to 94%  $U^{235}$  in the form of rods canned in stainless steel. The coolant (NaK) was present, but not flowing. Diagnostic experiments were in progress to deduce the basic cause of previously observed reactivity oscillations. A series of human errors occurred which resulted in an excursion which went beyond the original planned power level, and before the system could be physically scrammed, considerable damage was done to the core. The central part had melted and had, in general, sunk to the lower part of the core. Some of the material originally in the core had been forced into the upper and lower blankets. Apparently, the fast scram stopped the excursion before the reactivity exceeded prompt critical. The outer parts of the core, and, in particular, the can surrounding the core suffered no damage whatsoever.

By accepting the assumptions leading to the threshold model, discussed above, the total energy releases of systems discussed in this paper can be estimated without the need for a digital computer. In particular, the method applies to a sphere having, at time  $t = 0$ , an outer radius  $b$ , a uniform density  $\rho$ , and a parabolic energy production distribution with an  $\exp(\alpha t)$  time dependence.

We must make the assumption (believed to be a good one) that neglecting the decrease of  $\alpha$  during disassembly is compensated for by discarding the energy produced after the system has returned to critical.

Defining  $r = R(t = 0)$ , we write the energy per unit mass as:

$$E(r, t) = E_0(1 - qr^2/b^2) \exp(\alpha t). \quad (10)$$

$E_0$  is determined by the power level at  $t = 0$ ;  $q$  is chosen to fit the flux distribution. We are looking for the total energy:

$$Y = ME_0(1 - 3q/5) \exp(\alpha t_c), \quad (11)$$

where  $M$  = core mass and  $t_c$  = critical time.

If we take the pressure to be:

$$P(r, t) = \max[0, \rho(\gamma - 1)\{E(r, t) - Q^*\}], \quad (12)$$

then the Lagrangian equation of motion:

$$d^2R/dt^2 = -(\partial P/\partial R)/\rho \quad (13)$$

can be integrated immediately, giving  $R(r_c) = r$  as a function of  $E_0 \exp(\alpha t_c)$  and  $Q^*$ .

Following Bethe and Tait,<sup>1</sup> we can relate a function of known nuclear constants to an integral involving  $R(t_c) = r$  and thus to  $E_0 \exp(\alpha t_c)$  and  $Q^*$ . If  $Q^*$  can be determined by thermodynamic information or by experiment, this leads to the evaluation of  $Y$ .

We must distinguish the following two cases: (1)  $E(r, t_c) < Q^*$  for some  $r \leq b$  (positive pressure has not reached the outside); (2)  $E(r, t_c) \geq Q^*$  for all  $r \leq b$ .

For case (1), we find that

$$Y = MQ^*(1 - 3q/5)/(1 - qx^2), \quad (14)$$

where  $qx^2$  is the solution of the transcendental equation  $qx^2G(qx^2) = H^{2/9}$ . Here

$$H = \frac{63(1+f)}{32f\Sigma v} \frac{\alpha^3 b^2}{qQ^*(\gamma-1)}; \quad (15)$$

$f$  is the excess number of prompt neutrons per average collision,  $\Sigma$  is the macroscopic transport cross section for density  $\rho$ , and  $v$  is the average neutron velocity.  $bx$  is the radius at which  $E = Q^*$ .  $G(y)$  is a smooth function with slope 46/99 at the origin and infinite at  $y = 1$  (see the tabulation below).

$y$	$G(y)$
0	1.0000
0.2	1.1075
0.4	1.2576
0.6	1.4912
0.7	1.6728
0.8	1.9509

The equation can be solved readily by graph and slide rule.

For case (2),

$$Y = MQ^*(1 - 3q/5)\lambda, \quad (16)$$

where  $\lambda$  satisfies the somewhat more complicated equation

$$\lambda - 5B(q) \ln[(1-q)\lambda] = 4q^{-5/2}\{H - [qG(q)]^{9/2}/63 + 1/(1-q)\}, \quad (17)$$

where

$$B(q) = q^{-3/2}[\frac{1}{2} \ln(1+q^{1/2}) - \frac{1}{2} \ln(1-q^{1/2}) - q^{1/2} - \frac{1}{3}q^{3/2}]. \quad (18)$$

Although formidable in appearance, the equation is of the form  $\lambda - a \ln(b\lambda) = c$  and can be solved on a log slide rule, quickly except near  $\lambda = 1/(1-q)$ .

Specifically, this scheme has been used to estimate burst yields as a function of excess reactivity over prompt critical for the bare 66 kg core and the reflected 147 kg core discussed above and illustrated in Fig. 9. The assumed  $Q^*$ 's were  $2.2 \times 10^9$  erg/gm and  $5 \times 10^9$  erg/gm, respectively, chosen to coincide with the thresholds in the digital computation. To facilitate comparison, the results of the two methods for these cores are displayed again in Fig. 11 where we plot total burst yield against excess reactivity. The agreement is satisfactory.

## APPENDIX

The equation of state depends on the magnitude of the specific volume  $V$  ( $\text{cm}^3/\text{gm}$ ) and, in some cases, the temperature  $\theta$  (volts).

For the region in a  $P$ - $V$  diagram where  $V/V_0 > 1.33$  ( $V_0 = 1/18.75$ ) and for all  $\theta$ , a Van der Waals' function is used. Following Brout<sup>10</sup> we accept the critical values  $T_c = 14,000^\circ\text{K}$ ,  $V_c = 40 \text{ cm}^3/\text{mole}$ . We have used  $P_c = 1.0899 \times 10^{10}$  dynes/cm<sup>2</sup>. The Van der Waals' function is then:

$$P_1 = P_c \frac{\frac{8\theta}{3\theta_c}}{\left(\frac{V}{V_c} - \frac{1}{3}\right)} - \frac{3}{\left(\frac{V}{V_c}\right)^2}. \quad (19)$$

This function is not sufficient in that special provision must be made for points within the liquid-vapor saturation curves. The liquid saturation curve is taken to be

$$P_2 = -2.008343 \times 10^{-2} + 1.895703 \times 10^{-2}(V/V_0) - 2.89978 \times 10^{-3}(V/V_0)^2, \quad (20)$$

and the vapor saturation curve is

$$P_3 = 1.0953495 \times 10^{-2} - 1.6671762 \times 10^{-5}(V/V_0). \quad (21)$$

The pressures obtained from Eq. 20 and Eq. 21 are in megabars. Pressures within the  $P$ - $V$  area defined by Eqs. 20, 21 and  $P = 0$  are given by:

$$P_4 = 46.3P_c \exp\left(-3.8376 \frac{\theta_c}{\theta}\right). \quad (22)$$

Implicit in Eq. 22 is the Clapeyron-Clausius equation and a latent heat of vaporization of  $1.067 \times 10^5$  cal/mole. The choice of which function to use is made by the computing machine. The necessary information for a logical decision is incorporated in the code.

The equation of state for the region in a  $P$ - $V$  diagram where  $1.0 \leq V/V_0 \leq 1.33$  is divided into three sub-regions defined by the magnitude of the pressure. These functions are:

$$P_5 = -5.45649 + 0.27846\theta + 2.873 \times 10^{-2}\rho, \quad (23)$$

$$P_6 = -2.99148 + 24.7087\theta, \quad (24)$$

and

$$P_7 = 0.56440935 + 0.27846\theta - 0.5386875(V/V_0). \quad (25)$$

These three functions rather crudely represent regions of a solid (Eq. 23), a liquid (Eq. 25) and a transition region (Eq. 24). The form of Eq. 23 and Eq. 25 was chosen to match the apparent form as seen for various metals that were studied by Walsh *et al.*<sup>17</sup> Equation 24 was constructed by assuming (a) a latent heat of fusion ( $4.7 \times 10^8$  cal/mole), (b) a volume change of  $\Delta V = 0.00266$  cm<sup>3</sup>/gm, and (c) that  $P = \text{const.} \times E$  throughout the phase change. The logical decisions

necessary for a choice between Eqs. 23, 24 and 25 were incorporated into the code.

For the region where  $V/V_0 < 1.0$ , Eqs. 23, 24 and 25 were used again after multiplication by  $(V_0/V)^2$ . This modification is necessary to allow for the rapid rise in pressure with decreasing volume as seen by Walsh *et al.*<sup>17</sup>

A final restriction on the equation of state is required to limit tensions that may develop through application of Eq. 23. An upper limit to the dynamic tensile strength of uranium has been estimated to be between 0.3 and 0.5 megabars.<sup>18</sup> We have arbitrarily taken 0.3 megabars at room temperature (17°C). We have assumed further that this quantity decreases linearly with increasing temperature to zero at 4096°K. This function is defined by

$$P_8 = -0.3228538 + 0.9146\theta. \quad (26)$$

The calculation is coded such that if a pressure in a given region is found to be numerically more negative than Eq. 26 for the same temperature, the pressure is arbitrarily set to zero. Furthermore, the code forbids the particular region to support any negative pressures at any future time, although positive pressures are allowed.

The heat capacity is assumed to be a function of temperature only. For  $\theta \leq 8.1 \times 10^{-2}$  volt,<sup>8</sup>

$$C_v = 1.234619 \times 10^{-2} - 1.02858 \times 10^{-2}\theta + 1.809525\theta^2. \quad (27)$$

For  $\theta > 8.1 \times 10^{-2}$ , with one exception noted below (Eq. 29), we use

$$C_v = 1.84 \times 10^{-2}. \quad (28)$$

The one exception is found when the code makes use of Eq. 23 for pressure. When a given region is found to require Eq. 23, the heat capacity is given by

$$C_v = 1.6273. \quad (29)$$

The units associated with these heat capacities are  $10^{12}$  ergs/gm volt.

## REFERENCES

1. H. A. Bethe and J. H. Tait, *An Estimate of the Order of Magnitude of the Explosion when the Core of a Fast Reactor Collapses*, US-UK Reactor Hazard Meeting, RHM (56)/113, April (1956).
2. R. E. Peterson and G. A. Newby, *An Unreflected U<sup>235</sup> Critical Assembly*, Nuclear Sci. and Eng. 1, 112 (1956).
3. J. Codd, L. R. Shepherd and J. H. Tait, *The Physics of Fast Reactors*, Progress in Nuclear Energy, Pergamon Press Ltd., London, Series I, Vol. 1 (1956).
4. B. C. Carlson, *The S<sub>n</sub> Method and the SNG and SNK Codes*, Los Alamos Scientific Laboratory Report, LAMS-2201 (1958).
5. H. C. Paxton, *Critical Masses of Fissionable Metals as Basic Nuclear Safety Data*, Los Alamos Scientific Laboratory Report, LA-1958 (1955).
6. T. F. Wimett, *Time Behavior of Godiva Through Prompt Critical*, Los Alamos Scientific Laboratory Report, LA-2029 (1956); see also T. F. Wimett and J. D. Orndoff, *Applications of Godiva II Neutron Pulses*, P/419, Vol. 7, these Proceedings.
7. J. D. Orndoff, *Prompt Neutron Periods of Metal Critical Assemblies*, Nuclear Sci. and Eng. 2, 450 (1957). The Rossi alpha quoted in this article is  $-1.03 \times 10^6$  sec<sup>-1</sup>. It was obtained indoors and the experiment was affected somewhat by scattering from walls and the floor. A better value, obtained outdoors, 20 ft from the ground, is  $-1.10 \times 10^6$  sec<sup>-1</sup>.
8. J. J. Katz and E. Rabinowitch, *The Chemistry of Uranium, Part I*, p. 146, McGraw-Hill Co., Inc., New York (1951).
9. J. R. Dietrich, *Experimental Investigation of the Self-Limitation of Power During Reactivity Transients in a Subcooled, Water-Moderated Reactor*, Argonne National Laboratory Report, ANL-5323 (1954).
10. R. H. Brout, *Equation of State and Heat Content of Uranium*, Atomic Power Development Associates, Inc., Report APDA-118 (1957).

11. L. J. Koch, H. O. Monson, D. Okrent, M. Levenson, W. R. Simmons, J. R. Humphreys, J. Housnes, V. C. Jankus and W. B. Loewenstein, *Hazard Summary Report, Experimental Breeder Reactor II*, Argonne National Laboratory Report, ANL-5719 (1957).
12. W. E. Nyer, S. G. Forbes, F. L. Bentzen, G. O. Bright, F. Schroeder and T. R. Wilson, *Experimental Investigations of Reactor Transients*, Atomic Energy Comm., Research and Development Report, IDO-16285 (1956).
13. K. Fuchs, *Efficiency for Very Slow Assembly*, Los Alamos Scientific Laboratory Report, LA-596 (1946).
14. G. E. Hansen, *Burst Characteristics Associated with the Slow Assembly of Fissionable Materials*, Los Alamos Scientific Laboratory Report, LA-1441 (1952).
15. R. O. Brittain, *Analysis of the EBR-I Core Meltdown*, P/2156, Vol. II, these Proceedings.
16. W. H. Zinn, *A Letter on EBR-I Fuel Meltdown*, *Nucleonics*, p. 35 (June 1956). See also *Nucleonics*, p. 84 (January 1957).
17. J. M. Walsh, M. H. Rice, R. G. McQueen and F. L. Yarger, *Shock-Wave Compressions of Twenty-Seven Metals, Equations of State of Metals*. *Phys. Rev.*, *108*, 196 (1957).
18. R. D. Cowan, private communication.